International Journal of Fluid Power, 2015
Vol. 16, No. 1, 25–34, http://dx.doi.org/10.1080/14399776.2015.1017360

Taylor & Francis
Taylor & Francis Group

Experimental and numerical investigation of fluid flow of truncated conical poppet valve

Jalal M. Jalil[a]*, Sabah T. Ahmed[b], Yiqin Xue[c] and Safaa A. Ghadhban[d]

[a]*Electromechanical Engineering Department, University of Technology, Baghdad, Iraq;* [b]*Mechanical Engineering Department, University of Technology, Baghdad, Iraq;* [c]*Institute of Technology, Machine Department Middle Technical University, Baghdad, Iraq;* [d]*Commission of Technical Education, Baghdad, Iraq*

(*Received 15 September 2014; accepted 6 February 2015*)

Poppet valve development requires study of the complex flow inside it. This needs an advanced technology, such as particle image velocimetry (PIV) technique and CFD flow simulation. The main keys of this work are experimental investigation of the flow structure through a truncated conical poppet valve by using PIV technique. A numerical model of the valve is validated using experimental results. This validation gives the ability to modify the valve geometry and improve the flow structure, furthermore, and minimize the energy losses. The experiments have been done using the three flow rate values (Q) (25, 35, 45) L/min, each of them with three poppet displacements (Xv) (3.5, 5.5, 7.5) mm. The vortex radius and intensity, which is an indicator of losses magnitude, increased with the increasing of flow rate and decreasing of poppet movement Xv. The experimental results showed a good agreement with the numerical one, beyond some difference for flow out of the metering area. The three-dimensional effects may be the reason of this difference. The results provide good information to design process.

Keywords: hydraulic; CFD; poppet; valve; PIV

1. Introduction

A poppet valve is a seating type valve in which the moving element or poppet, usually spherical or conical in shape, moves in a direction perpendicular to the axis of its seat. Poppet is to be found in relief valves, pressure regulators, and selectors. The flow inside the poppet valve is a complex process that is strongly dependent on the details of the valve geometry, the fluid properties, and the operating conditions. Separation and reattachment of jets can have a profound effect on the flow pressure and force characteristics (Johnston *et al.* 1991). Poppet valve has been studied by many researchers. Johnston *et al.* (1991) conducted a series of experiments to explore the flow coefficients and steady-state flow force for poppet and disk valves. The conclusion was that, at the small opening, the fluid characteristics of the poppet valves with angled seats have much more intense relationship with the reattachment of the flow jet to the valve seat than that of those with sharp-edged seats. Vaughan *et al.* (1992) performed 2-D CFD simulation of the steady turbulent incompressible flow through a poppet valve with conical seat to investigate the discharge coefficients and force characteristics. The results showed good quantitative and qualitative agreement with experiment when no flow separation occurred. KazumiIto and Inoue (1993) calculated the pressure distribution in a poppet valve based on streamline coordinate. The numerical results showed that the shear forces were less than 6% of the pressure forces. Mokhtarzadeh-Dehghan *et al.* (1997) described the finite element study of a laminar flow of oil through a hydraulic pressure relief valve used in a variable compression ratio piston of an internal combustion engine. It was found that the forces acting on the valve poppet increased with the flow passage gap. Watton and Bergada (2004) developed a new set of equations giving insight into the laminar flow and pressure distribution across poppet valves with large cone-shaped seats and small valve openings. The equations were a useful design tool for linear pressure/flow applications. Zhanghua and Yingfeng (2004) studied the cone throttle valve used in oil field to solve many failure problems, such as valve rod fatigue fracture and poor linear adjusting. It was found that the sharp change in flow direction results in a great energy loss. They presented a wedge throttle valve and its life was 5–7 times that of the cone valve. Bernad *et al.* (2005) confirmed the results obtained numerically by the experimental results and showed that the velocity profiles in the metering sections are strongly influenced by the three-dimensional effects of the flow. Bernad and Susan-Resiga (2012) numerically compared liquid flow with two phases flow. It was shown that the liquid flow model can correctly predict the cavity radius. Tongle and Zhang (2008) numerically analyzed and simulated the fluid flow in the throttle poppet valve. The design of poppet was modified to minimize the energy loss by elongating the poppet with the same angle to get a tapered head with no changed configuration of poppet and seat. Gao *et al.* (2009) showed, by both results of numerical simulation and particle image velocimetry (PIV) experimental, that

*Corresponding author. Email: jmjalil@uotechnology.edu.iq

there are three main areas in the spool valve where vortex is formed. Washio *et al.* (2010) experimentally investigated possible ways for cavitation to be generated in liquid flows of poppet valve. They concluded that as the cavities ware generated, the flow pulsation resulted in a self-excited vibration of the poppet supported by a spring. Yang *et al.* (2011) investigated experimentally and theoretically the flow characteristics of water hydraulic poppet valve with a sharp-edged seat. A simple theoretical model was developed to describe the pressure distribution on the poppet conical surface. Lazowski (2012) performed a numerical analysis of flow though poppet valve. Two-dimensional and Three-dimensional valve model was considered. The difference between 2-D and 3-D characteristics increases for large values of volumetric rate flow because of the growth of viscous forces between fluid layers. Taghinia-Seydjalali and Siikonen (2013) carried out a numerical investigation using the RNG-k-ε turbulent model to study the effect of the shape of the valve (conical and ball head). The results showed that the velocity value in the ball head case tends to decrease more slowly and its direction follows the head curve. Liu *et al.* (2014) presented a numerical two-phase flow model combined with the Realizable k-ε turbulent model for simulation of flow around a fixed-cone valve. The function of the valve for energy dissipating was pointed out by analyzing the computed pressure field and velocity field of the valve.

The aim of this study is to investigate the influence of poppet valve opening and passing flow rate on the flow structure, such as velocity and vortex formation. This aim can be captured using PIV technique, which is a powerful whole-field velocity measuring tool, utilized to get the flow field along the inlet passage and the outlet passage of a poppet valve simultaneously. It does not disturb the flow as in hot wire. In order to capture the flow field inside the valve through PIV measurements, a valve model has been equipped with an optical access. A numerical model of the valve can be used to simulate the flow and validated using the experimental results.

2. Geometry and mathematical model

Poppet valve development requires study of the complex flow inside it. This needs an advanced technology, such as CFD flow simulation. The flow inside poppet valve is almost outflow (flow to open) configuration. The design of truncated poppet valve depends on its function, such as relief valve and check valve. The geometry of typical truncated poppet valve is shown in Figure 1. Practically, the poppet is moved and reached balanced point as a result of one or more of applied forces, such as spring force, flow force and pilot force. The steady, incompressible and viscous flow of a fluid through the poppet valve is described by the Navier–Stokes (NS) equations. The flow is turbulent and described using k-ε model. The general form of NS equations can be written as (Patankar 1980):

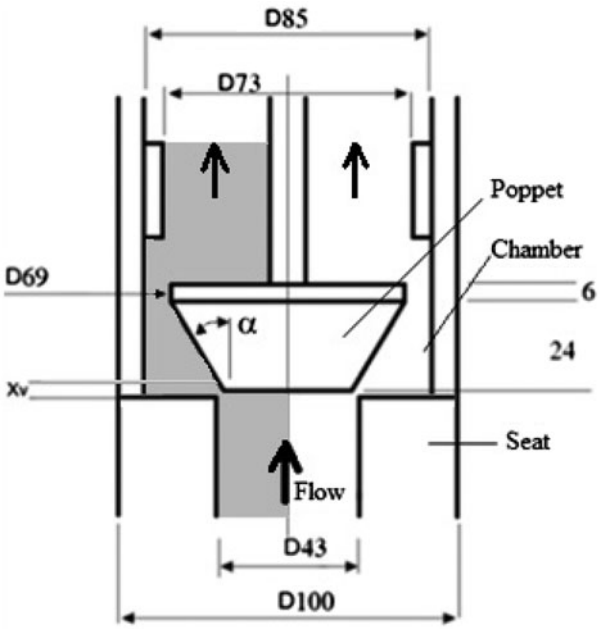

Figure 1. Valve geometry.

$$\frac{\partial(\rho u j\phi)}{\partial x_j} = \frac{\partial}{\partial x_j}.\left[\Gamma eff\frac{\partial\phi}{\partial x_j}\right] + S\phi \qquad (1)$$

where ϕ is the dependent variable and S_ϕ is the source term. Γ_ϕ represents the diffusion coefficient. Table 1 gives the expressions of S_ϕ for each ϕ.

3. Fluid flow in poppet valve by finite volume method

A numerical technique (CFD) by using (FORTRAN 90) has been developed to solve the governing partial differential equation of the mathematical model in two dimensions to simulate and predict the flow velocity and pressure distribution in the poppet valve. In present work, a collocated arrangement of orthogonal grid is chosen. The governing equation is discretized using the finite volume method. The pressure and velocity coupling equation is solved using the SIMPLE algorithm. The smoothing pressure correction is used to match the collocated arrangement (Date 2005). The problem is solved for the left half of the valve due to symmetry as shown in Figure 1.

The following assumptions and boundary conditions are assumed:

Table 1. The expressions of S_ϕ for each ϕ.

Equation	Φ	Γ_ϕ	S_ϕ net source
Continuity	1	0	0
x-momentum	$u1$	μ_e	$-\frac{\partial P}{\partial x_1} + \rho B_1 + Su_1$
y-momentum	$u2$	μ_e	$t - \frac{\partial P}{\partial x_2} + \rho B_2 + Su_2$
Turbulence Energy	K	Γ_k	G-$\rho\varepsilon$
Dissipation rate	ε	$\Gamma\varepsilon$	$\frac{\varepsilon}{\kappa}[C_1 G - C_2\rho\varepsilon]$

(1) Steady-state flow.
(2) Newtonian and incompressible fluid with constant properties.
(3) Turbulent and adiabatic flow.
(4) Axisymmetrical about the centerline of the valve (two-dimensional)
(5) The inflow velocity is fully developed.
(6) Turbulent intensity (TI) = 10% (Bernad *et al.* 2005), thus, $k_{in} = 0.1u_{in}^2$, and $\varepsilon_{in} = C_\mu \rho k^2/\mu_t$
(7) Back pressure is specified as ($p = 0$), where for the same flow rate one should expect practically the same pressure drop.
(8) The gradients for symmetric wall of all the variables are set to zero ($\frac{\partial \phi}{\partial \mathbf{n}} = 0$).
(9) Standard wall functions are used to estimate the viscous effect close to walls.

The computational grid of flow around the valve is generated by Fortran 90, is shown in Figure 2. The way of checking whether the solution is grid independent or not is to create a grid with more cells to compare the solutions of the two models. A computational mesh of (134 × 85) cells was employed after grid independence tests were performed. The poppet is set at different positions and different inlet flow rates. The valve openings related to three different poppet positions are $Xv = 3.5$, 5.5, and 7.5 mm. In order to apply orthogonal grids to solution domains with inclined boundary of poppet, the boundaries have to be approximated by staircase-like steps. This approach has been used, and required special arrays have to be created. The computer code needs to be changed for each problem of poppet valve. The inlet condition is set similarly to experimental ones, where the inlet flow rate cases are $Q = 25$, 35 and 45 L/min.

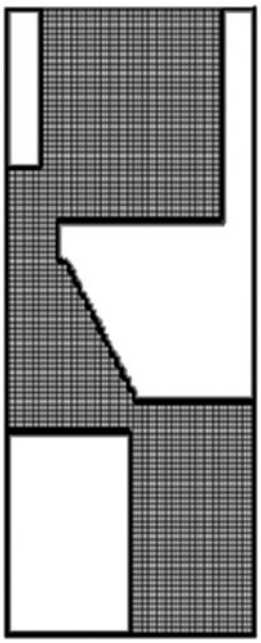

Figure 2. Grid generation of CFD.

The implementation of wall boundary conditions in turbulent flows required the evaluation of parameter $y^+ = (y_p/v)\sqrt{(\tau_w/\rho)}$,where (τ_w) is the wall stress and (y_p) is the distance of the near wall node (P) to the solid surface. The near-wall flow is taken to be laminar if ($y^+ < 11.63$). The flow is turbulent and the wall function approach can be used if ($y^+ > 11.63$).

4. Experimental work

A test rig for the present investigation has been constructed at Fluid Power Laboratory of Mechanical Engineering Department/Cardiff University to investigate the flow characteristics through a truncated conical poppet valve. The schematic of the test rig is shown in Figure 3.

4.1 Experimental device

The experimental test section consists of transparent elements made of acrylic material. The model is integrated in a fluid circulation system with a tank for containing fluid with tracing particles. A centrifugal pump, driven by electric motor, is used to provide energy to the circulation fluid. The used fluid is water ($\rho = 0.998$ g/cm^3, $v = 0.01011$ cm^2/s). The flow rate entering the model is measured by using an electromagnetic flow meter with an accuracy of 0.1% for the measured ranges.

The poppet has an angle of $2\alpha = 60°$. The upstream and downstream diameters of the test section are 43 and 85 mm, respectively. The valve is also equipped with two pressure transducer taps before and after metering area to measure the pressure difference. The poppet part position Xv can be adjusted by adjustable screw to allow different geometrical cases ($Xv = 3.5$, 5.5, and 7.5 mm) to be studied. Also, the flow rate is controlled using throttle valve to allow different flow rates ($Q = 25$, 35, 45 L/min) through valve to be investigated. Another throttle valve is used to increase the back pressure and thus avoid cavitation, which causes reflection of laser light and incorrect results.

A square cross-section box, filled with water, was fixed around the valve body for its optimal optical access in order to avoid the astigmatismeffect due to the curved surface of the valve pipe.

4.2 PIV system

PIV technique is a whole field velocity measuring tool. It is used to measure the fluid dynamic characterization, such as air flowing around a car, water running through hydroelectric turbine, blood flow, etc. The principle of PIV is to measure the distance Δs of tracing particles moving with the fluid during a known time interval Δt, then the velocity u is calculated by Adrian (1991):

$$u = \frac{\Delta S}{\Delta t} \tag{2}$$

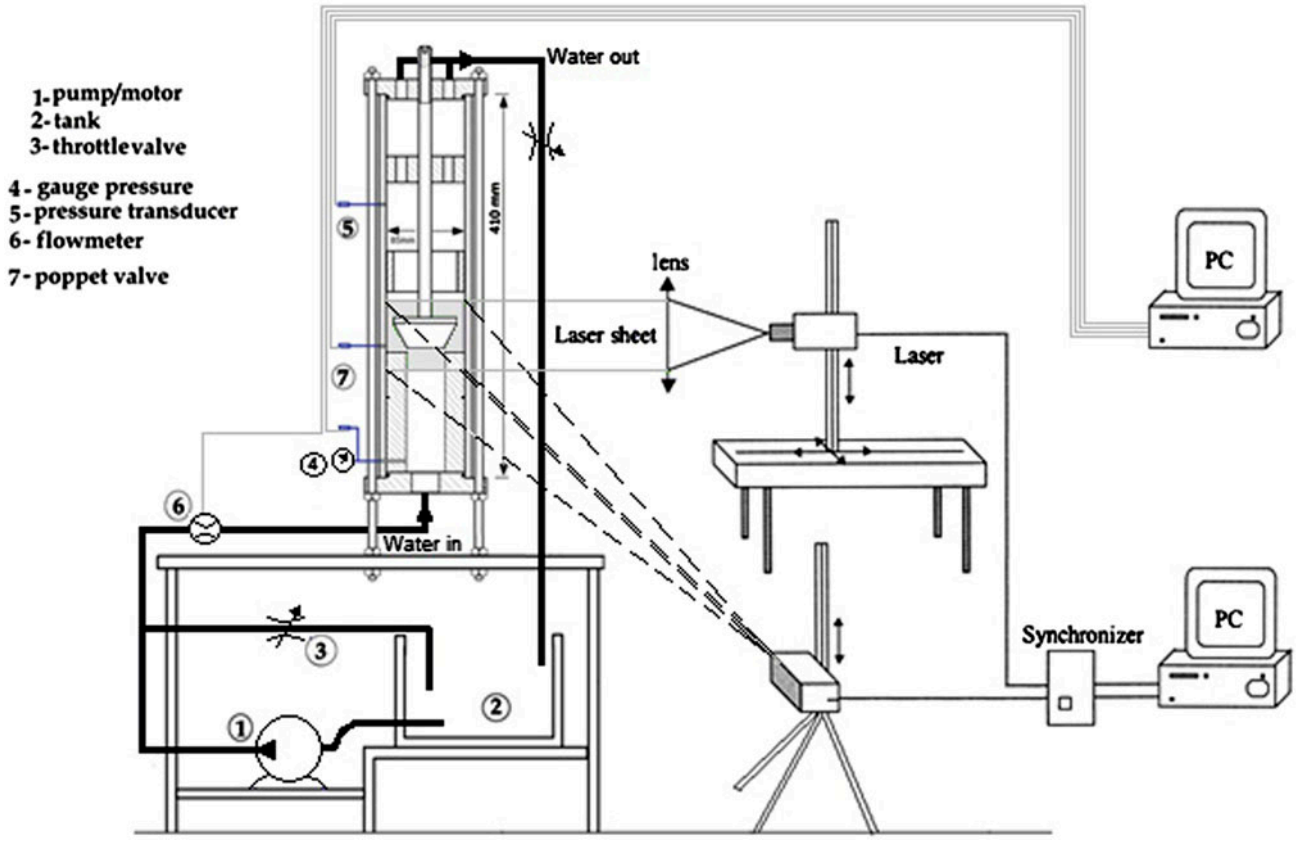

Figure 3. Schematic of test rig.

A typical PIV system comprises several subsystems: a tracer particle seeded flow, a high sensitivity CCD camera, a light source for illumination of the tracer particles on a chosen plane, and a computer for data acquisition and extraction of information of tracer particle positions (Prasad 2000).

A PIV system from TSI (2011) has been utilized for the measurements. It consists of a double-pulsed Neodymium-doped yttrium lithium fluoride (Nd: YLF) laser with a wavelength of 527 nm. Two lenses (convex and concave) are used to convert the laser beam into a 2-D laser light sheet with average thickness of 1.5 mm. It is employed to illuminate a vertical plane which sections the valves into approximately similar halves. Experiments were carried out at vertical poppet valve because of limitations of PIV system installation (Figure 3). The energy of each laser is 150 mJ.

The FASTCAM-APX RS high speed camera system has been used for acquisition of double images from which velocity fields are determined. The camera has a resolution 1024 × 1024 pixel and is equipped with an objective of 60 mm.

The flow has been seeded by glass spherical particles. Their sizes are (8–12 μm) and density 1.016 g/cm^3. The particles are small enough to follow the flow, and specific gravity is close to water so that the particle sedimentation can be neglected. Figure 4 shows the picture of PIV system installed for rig of valve model.

4.3 Data processing

The data of image processing have been realized by 4G-Insight software from TSI (2011). The velocity vectors were calculated by cross-correlating two pictures taken 0.5–1 ms apart. An interrogation window of 32 × 32 pixels without overlapping is found suitable for the current work due to the maximum displacement of the particles from one frame to another, and the camera is not able to focus smaller regions. The time separating two pulses was chosen as follows:

(1) The maximum pixel displacement should not exceed quarter of minimum dimension of interrogation spot (TSI incorporated INSIGHT 4G 2011), so pixel distance (Dis. in pixel) < $\left(\frac{32}{4} = 8\right)$.
(2) The maximum velocity for example at $Xv = 5.5$ mm and $Q = 35$ L/min is estimated, depending on continuity equation, to be 1.0 m/s.
(3) The calibration for all cases was (20 mm = 110 pixel). So, Dis = 1.45 mm
(4) The time between two pulses < Dis/velocity = 1.45 ms
(5) Thus, the suitable choice of time apart was 1000 μs

The cross-correlation function was computed by performing two-dimensional FFT. Its peak was designated by using a Gaussian scheme in both directions of the

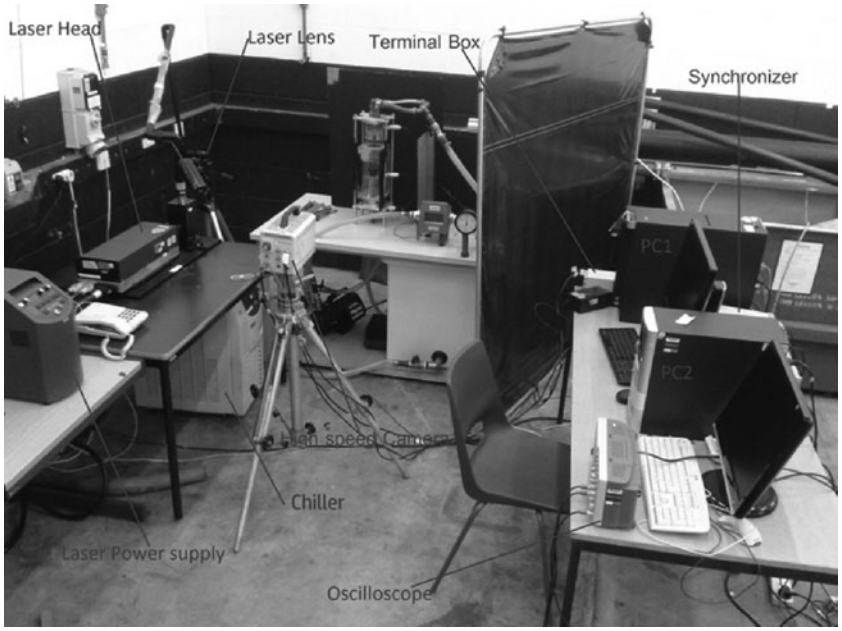

Figure 4. PIV system picture.

image plane, in order to increase its accuracy. Care has been taken during experiment to have adequate particles in each interrogation window. It should contain (5–15) particle images, but avoid overseeding in which many particles overlap.

5. Results

To show the two-dimensional velocity field inside the valve using PIV system, the laser light sheet was focused in the middle of the test section. The PIV camera was directed to the left part of the valve, around the region of the metering area. The tests were performed with three positions of poppet (3.5, 5.5, and 7.5 mm), each of them with three types of flow rate (25, 35, and 45 L/min). The experimental steady-state results obtained from PIV system for different openings and flow rates are demonstrated in Figures 5–13 in the form of velocity vectors plots. Table 2 lists the values of jet velocity at metering section at different poppet displacements and different flow rates. The Reynolds number (Re) is calculated based on inlet diameter ($d = 43$ mm), so, $\mathrm{Re} = \frac{ud}{\upsilon} = \frac{4Q}{\pi d\upsilon}$.

Generally, a great acceleration of the flow in the restricted section can be noticed, and the kinetic energy dissipation is also visible when the flow enters the discharge chamber. The figures of PIV results clearly show that there are two different types of patterns. For first type, there is one vortex generated as shown in Figure 11, for case $Xv = 3.5$ mm and $Q = 25$ L/min. It is formed near the corner of the chamber. It seems as large recirculation region and its intensity is being stronger with the decrease of the valve opening. Thus, the energy losses and flow fluid noise caused by vortex will be greater. In this pattern, the annular jet through poppet-seat slit

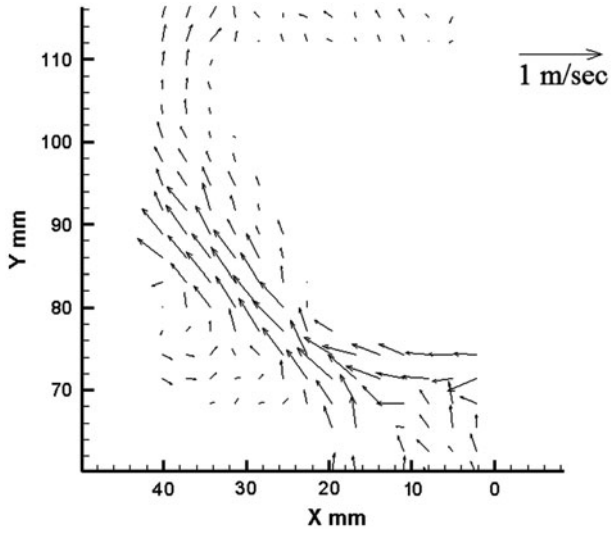

Figure 5. Velocity vectors of PIV results at $Xv = 7.5$ mm and $Q = 25$ L/min.

remains attached to the poppet surface, so the jet angle equals to the poppet angle. This is because of Coanda effect due to the pressure variation perpendicular to curved streamlines. For second type, there are two zones inside the valve, where vortices are generated as shown in Figure 5, for case $Xv = 7.5$ mm and $Q = 25$ L/min. One vortex is formed near the corner of the chamber and its behavior is similar to that of first pattern type. Another vortex is located between main flow and poppet surface and it is getting stronger with increasing of valve opening. In this pattern type, the jet angle is greater than poppet angle. Thus, the metering area (A) is greater which leads to a drop in the discharge coefficient (Cd).

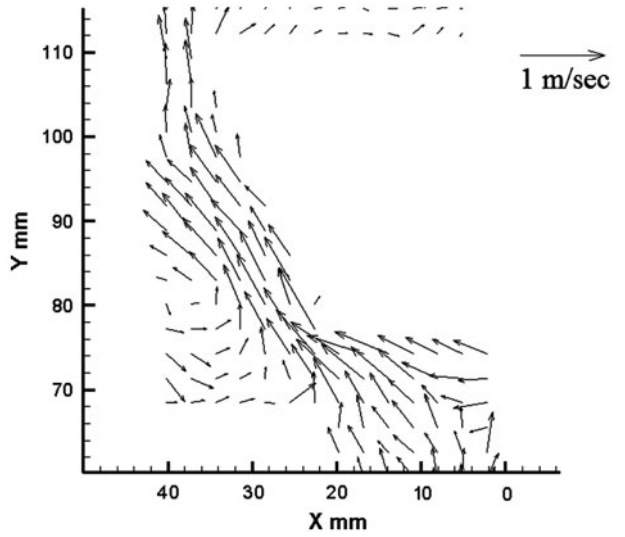

Figure 6. Velocity vectors of PIV results at Xv = 7.5 mm and Q = 35 L/min.

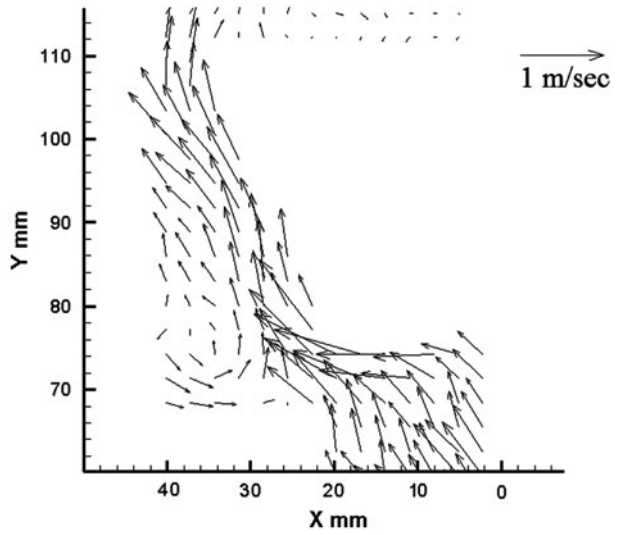

Figure 7. Velocity vectors of PIV results at Xv = 7.5 mm and Q = 45 L/min.

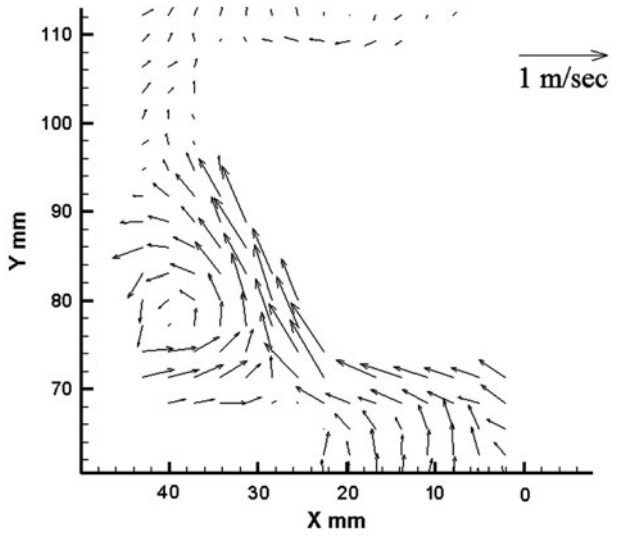

Figure 8. Velocity vectors of PIV results at Xv = 5.5 mm and Q = 25 L/min.

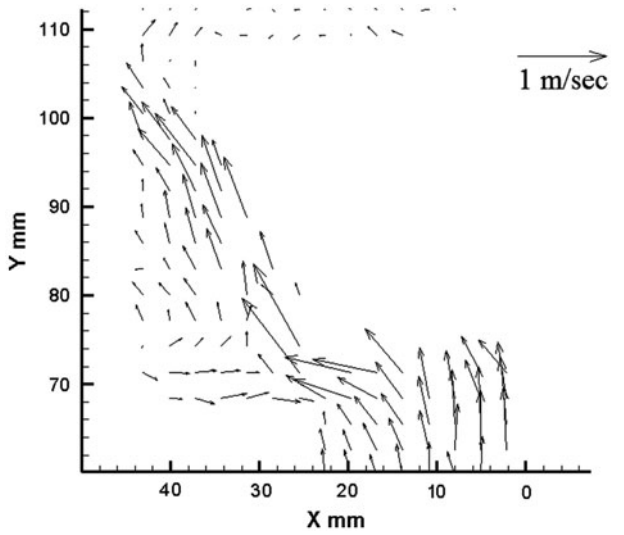

Figure 9. Velocity vectors of PIV results at Xv = 5.5 mm and Q = 35 L/min.

$$Cd = \frac{Q}{A}\sqrt{\frac{\rho}{2\Delta P}} \tag{3}$$

where Q is flow rate through the valve, ΔP is pressure drop across the valve, and ρ is fluid density. Figure 14 shows the pressure difference between sections before and after the metering region measured by pressure transducers with changing the flow rate pass the valve for different valve opening. The pressure differences increased with increasing of flow rate and decreased with increasing the valve opening. The flow is turbulent and the flow curves are nonlinear. The trend of discharge coefficient with flow rate for different poppet displacement is represented in Figure 15. It is noticed that the discharge coefficient is approximately constant as flow rate increases. It also decreases as poppet displacement increases because the fluid undergoes higher change in direction in passing through the orifice, and hence higher contraction of the jet takes place as shown in PIV image.

The PIV results of truncated poppet valve obviously show that there are two different types of patterns. It was observed that the first pattern was found to be most prevalent for small openings. In this pattern, one vortex is formed in the corner of the valve chamber, and the jet attached to the valve poppet. The second pattern prevailed in situations of large openings and small flow rates. Two vortices are formed in these situations; one is big and similar to previous vortex and the second is

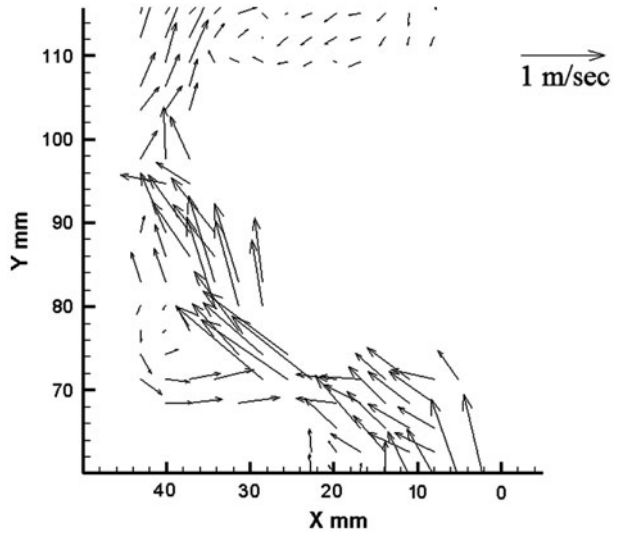

Figure 10. Velocity vectors of PIV results at Xv = 5.5 mm and Q = 45 L/min.

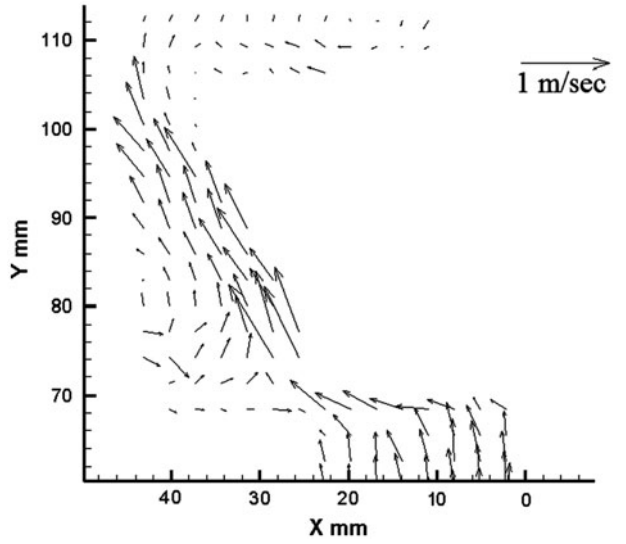

Figure 11. Velocity vectors of PIV results at Xv = 3.5 mm and Q = 25 L/min.

small and formed between main flow and poppet surface. The jet in the two patterns can be seen to flow past the orifice until it strikes the wall of the chamber. In the case of high flow rate and small opening (displacement Xv) as shown in Figures 10, 12, and 13, the particles, which are entered into inlet section and moved to the recirculation region, may not remain in the original injection plane. Also, the jet velocity is higher when the valve opening is smaller, thus the pressure drop across the metering area is higher. This means that much energy loss and flow fluid noise is produced when the valve opening is smaller. In PIV image shown in Figure 13, some velocity vectors seem lost. This is because either number of particles is insufficient or the time separated the laser pulses need to be adjusted to cover the velocities around the

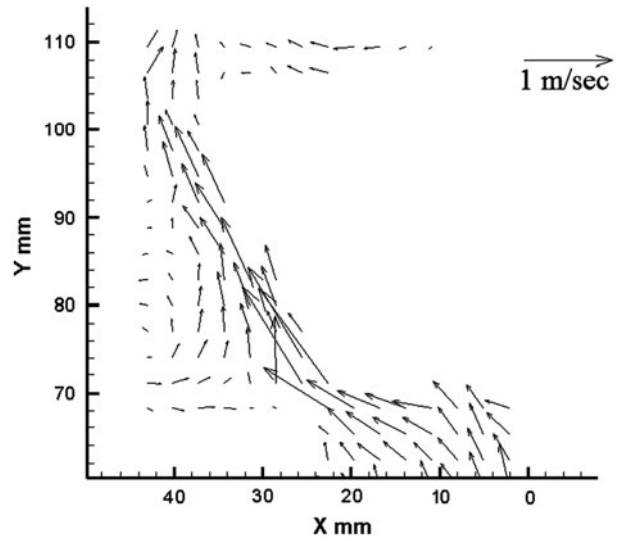

Figure 12. Velocity vectors of PIV results at Xv = 3.5 mm and Q = 35 L/min.

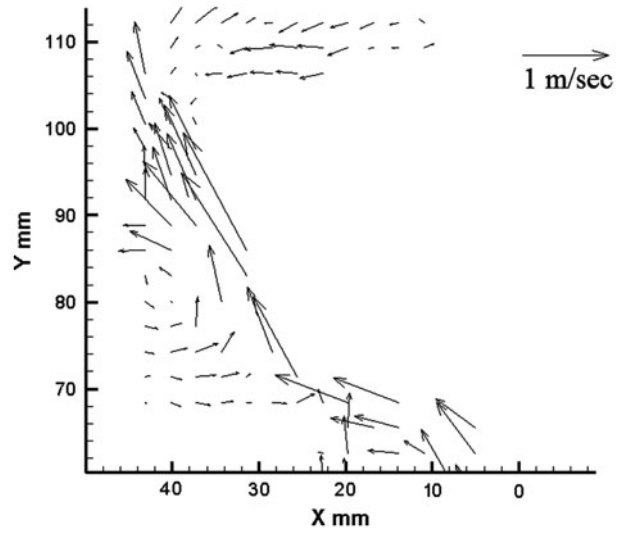

Figure 13. Velocity vectors of PIV results at Xv = 3.5 mm and Q = 45 L/min.

Table 2. Values of jet velocity at metering section for different conditions.

Xv mm	Flow rate Q (L/min)	Inlet velocity (m/s)	Reynolds no.	Jet velocity (m/s)
7.5	25	0.287	12210	0.561
7.5	35	0.402	17095	0.843
7.5	45	0.517	21980	1.102
5.5	25	0.287	12210	0.746
5.5	35	0.402	17095	1.057
5.5	45	0.517	21980	1.351
3.5	25	0.287	12210	0.961
3.5	35	0.402	17095	1.323
3.5	45	0.517	21980	1.535

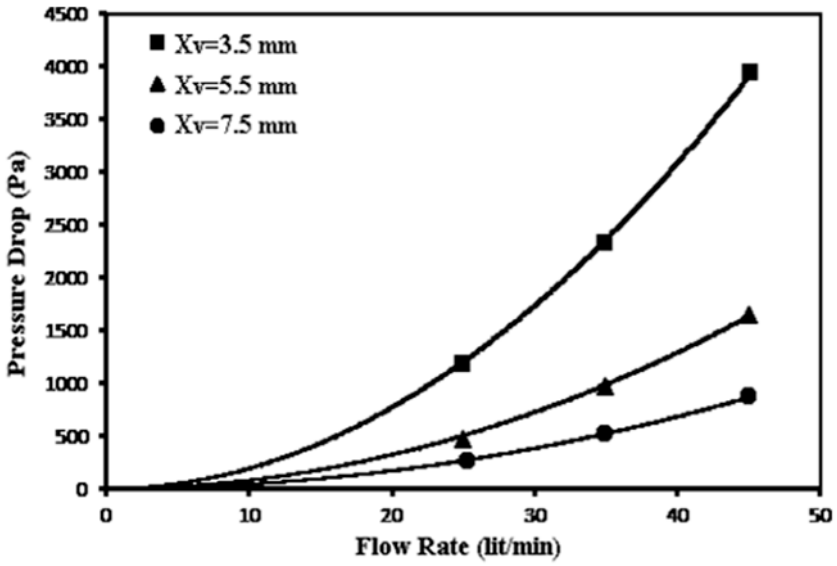

Figure 14. Pressure drop-flow rate relations for the valve at different valve openings and with the parabolic regression lines.

flow field. Generally, as the tracing particle displacement increases, the error increases because the number of correlated particles remaining in interrogation window of PIV grid decreases.

The velocity structure, numerically investigated, is shown in Figure 16, for case of $Xv = 7.5$ and $Q = 25$ L/min. The maximum velocity out of metering region is approximately the velocity observed in flow structure of experimental PIV results. For comparison purposes, both PIV results of Figure 5 and CFD results of Figure 16, which are with the same conditions, are used. In Figure 16, a vortex was observed which is little different from that in Figure 5 by CFD simulation. The vortex size by PIV is larger than that by CFD, but the intensity is weaker than that by CFD. The location of vortex center by PIV is about of (38, 78), while this position is about (37, 74) by CFD.

The differences are from the effects of the three-dimensional flow of the fluid within the test model. There are also some other factors that can bring errors to the PIV results, such as the inaccuracy in making the test model and the effectiveness of the image processing.

A modified design of truncated poppet valve is suggested to improve valve performance. Figure 17 demonstrate the velocity field of flow through modified valve. If the seat is sufficiently inclined, the jet is able to reattach itself to the seat within the clearance region. Significant pressure recovery can occur, resulting in an

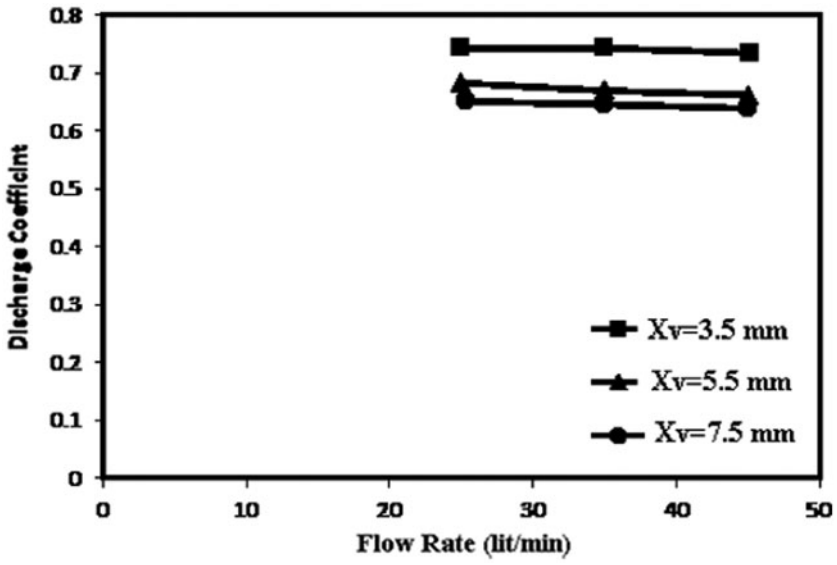

Figure 15. Variation of discharge coefficient with flow rate for different poppet displacement.

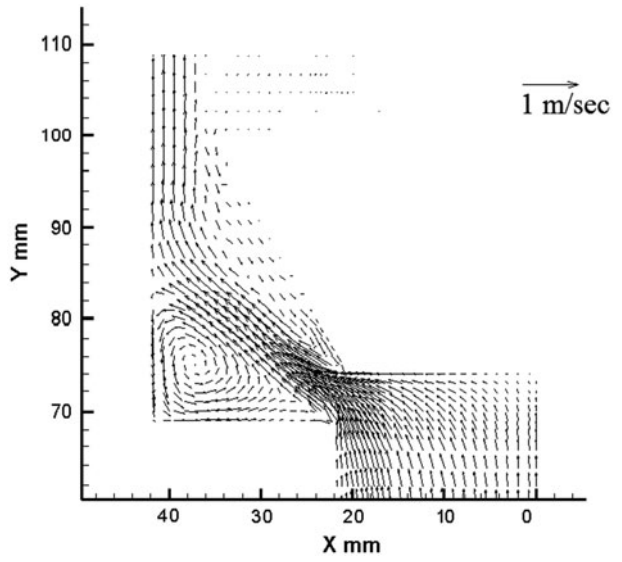

Figure 16. Velocity vectors of numerical results at $Xv = 7.5$ mm and $Q = 25$ L/min.

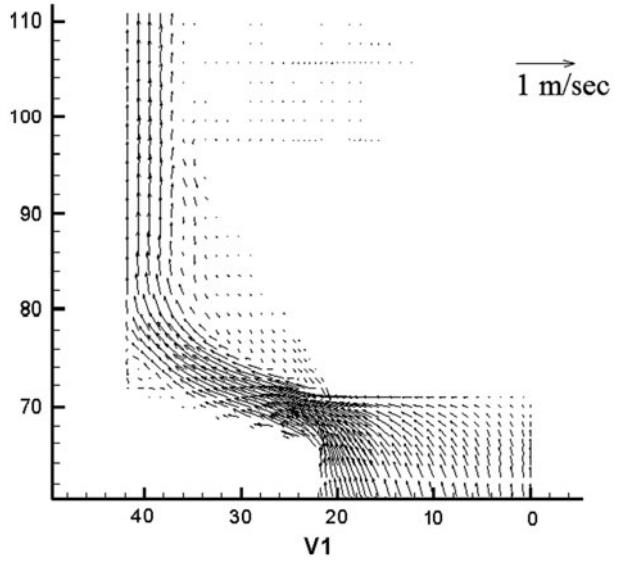

Figure 17. Velocity vectors of numerical results for modified design at $Xv = 7.5$ mm and $Q = 25$ L/min.

increased discharge coefficient Cd. By guiding the flow without the big vortex, energy is kept and fluid flow noise is minimized. The advantage of modified valve is the elimination of the big vortex which is an undesirable factor leading to the instability problems for the flow control of poppet in additional of noise generation.

6. Discussion and conclusions

This study shows that the built model of poppet valve is suitable for PIV investigations. The instrumentations and the used seeding particles are good for the study of the velocity profiles.

Each of PIV experiments and CFD simulation showed the flow structure through the poppet valve. Based on pattern type, one or two vortices are formed in the valve chamber. These vortices use energy from mainstream to keep the vortex rotating. This causes energy losses and noise generation of the flow. The radius and intensity of vortex is an indicator of losses magnitude.

The radius and intensity of the big vortex are increased with the increasing of flow rate. Also, as the valve opening is varied, the size and the intensity of the vortex vary accordingly. For big vortex, the smaller the valve opening is, the greater the vortex size and intensity are, while for small vortex, the larger the valve opening is, the greater the vortex size and intensity are.

A comparison between the experimental and predicated results for the velocity field through valve showed good qualitative agreement between the two. But, the experimental results depicted some difference, especially flow out of metering area, from numerical results. The three-dimensional effects are the reason of this case, because the CFD simulation uses the ideal axisymmetrical mathematical model, and the PIV experiments test model is no exactly two-dimensional in fact. Also the inaccuracy of PIV measurements is related to the particles hydrodynamic behaviors to follow the streamlines. It may be useful to mention here that although PIV technique is a powerful measuring tool, the accuracy of its results is affected by factors, such as laser sheet quality and image processing, therefore, researcher should give attention to these factors to get good results.

The results exhibited qualitatively that the velocity profiles out of the metering section are strongly influenced by the 3-D effects because the circumferential wall that limits the discharge chamber produces recirculation zones. Three-dimensional effects could be experimentally focused in future researches using 3-D stereo PIV system. This will allow quantitative analysis of expected helical motion.

Acknowledgments

The authors thank Cardiff University/School of Engineering and TSI Company for their corporation by supplying us the PIV system which made this work possible.

References

Adrian, R., 1991. Particle image velocimetry for experimental fluid mechanics. *Annual review fluid mechanics*, 23, 261–304.

Bernad, Sandor I., and Susan-Resiga, Romeo, 2012. Numerical model for cavitational flow in hydraulic poppet valves. Hindawi, Vol. 2012.

Bernad, Sandor, Muntean, Sebastian, Susan Romeo F., and Anton Ioan, 2005. Vorticity in hydraulic power equipment. Workshop on vortex dominated flows achievements and open problems. Timisoara.

Date, Anil W., 2005. *Introduction to computational fluid dynamics*. New York: Cambridge University Press.

Dianrong, Gao, Qiao, Haijun, and Lu, Xianghui, 2009. Finite element numerical simulation and PIV measurement of flow field inside metering-in spool valve. *Chinese journal of mechanical engineering*, 22 (1), 1–7.

Javad, Taghinia-Seydjalali, and Siikonen, Timo, 2013. Numerical investigation of flow in hydraulic valves with different head shapes. *Asian journal of scientific research*, 6 (3), 581–588.

Johnston, D.N., Edge, K.A., and Vaughan, N.D., 1991. Experimental investigation of flow and force characteristics of hydraulic poppet and disc valves. *Processing institution mechanical engineering*, 205, 161–171.

Kazumi, Ito, Koji, Takahashi, and Kiyoshi, Inoue, 1993. Flow in a poppet valve: computation of pressure distribution using a streamline coordinates system. *JSME international journal, series b: fluids and thermal engineering*, 36, 42–50.

Lazowski, Jacek, 2012. Flow analysis of hydraulic poppet control valve by means of computational fluid dynamics. *Journal of KONES powertrain and transport*, 19, 251–259.

Liu, Y.L., Bai, Ch.W., Wei, W.L., and Yang, X.F., 2014. Simulation of hydraulic characteristics around a fixed-cone valve. *Journal of chemical and pharmaceutical research*, 6 (1), 476–479.

Mokhtanadeh-Dehghan, M.R., Ladommatos, N., and Brennan, T.J., 1997. Finite element analysis of flow in a hydraulic pressure valve. *Elsevier Science Inc. Applied mathematical modelling*, 21, 437–445.

Patankar, Suhas V., 1980. *Numerical heat transfer and fluid flow*. New York: Hemisphere.

Prasad, A.K., 2000. Particle image velocimetry. *Current science*, 79 (1), 51–60.

Tongle, X.U., and Xinyi Zhang, 2008. Numerical analysis of fluid flow in the throttle poppet valve channel in precision machinery. *Proceedings of SPIE*, 7130, 71305I–1.

TSI incorporated, 2011. PIV system installation manual for INSIGHT software.

TSI incorporated INSIGHT 4G, 2011. Data Acquisition, Analysis, and Display Software Platform.

Vaughan, N.D., Johnson, D.N. and Edge, K.A., 1992. Numerical simulation of fluid flow in poppet valves. *Proceedings of the institution of mechanical engineers*, 206, 119–127.

Washio, S., Kikui, S., and Takahashi, S., 2010. Nucleation and subsequent cavitation in a hydraulic oil poppet valve. *Proceedings of the institution of mechanical engineers, part C: journal of mechanical engineering science*, 224, 947–958.

Watton, J. and Bergada J.M., 2004. A direct solution for flow rate and force along a cone-seated poppet valve for laminar flow conditions. *Proceedings of the institution of mechanical engineers, part I: journal of systems and control engineering*, 218, 197–210.

Yang, Yousheng, Wu, Jinjun, Fuzhou, Feng, and Zhu, Yuquan, 2011. Flow characteristics of throttle valve with sharp-edged seat. *IEEE International conference on fluid power and mechatronics (FPM), Beijing, 2011*, 218, 444–449.

Zhanghua, Lian, and Yingfeng, Meng, 2004. Fluid field analysis of high pressure throttle valve and it's structure improvement. Melbourne: International conference.